Structure, Conformation and Dynamics of 1,1,2,2-Tetracyano-3,3-dimethyl-4-(2′,2′-dimethylethenyl)cyclobutane as Detected by X-Ray and Multinuclear NMR Analyses

Dagfinn W. Aksnes,* Trond Brekke and Knut Maartmann-Moe

Department of Chemistry, University of Bergen, N-5007 Bergen, Norway

Aksnes, D. W., Brekke, T. and Maartmann-Moe, K., 1991. Structure, Conformation and Dynamics of 1,1,2,2-Tetracyano-3,3-dimethyl-4-(2′,2′-dimethylethenyl)cyclobutane as Detected by X-Ray and Multinuclear NMR Analyses. – Acta Chem. Scand. 45: 138–144.

The crystal structure of the title compound, a vinylcyclobutane derivative abbreviated to VCB, has been determined at 90 K by X-ray crystallographic methods. The crystals are orthorhombic, space group *Pcab* (No. 61), $a = 7.470(2)$, $b = 11.446(2)$, $c = 30.862(5)$ Å. The C–C bond lengths of the VCB ring are between 1.563 and 1.603 Å. The angle of pucker of the cyclobutane ring is 21.8°, and the C–C–C valence angles are between 87.9 and 89.9°. The conformation of the vinyl group is *anti*.

The ^{1}H, ^{13}C and ^{15}N NMR spectra of VCB in solution have been completely assigned using a combination of 1D and 2D experiments. The ^{1}H and ^{13}C NMR data show that the *anti* configuration of the vinyl group persists in solution. An analysis of the ^{1}H and ^{13}C spin–lattice relaxation times (T_1) of VCB is reported. The rotational correlation times for VCB are 23 ps for the overall motion and between 2.5 and 69 ps for the methyl reorientations. The rotations of the 3α and 3β methyl groups are considerably hindered.

The kinetics of the 2+2 cycloaddition reaction between tetracyanoethylene and 2,5-dimethyl-2,4-hexadiene to give the vinylcyclobutane derivative (henceforth called VCB) depicted in Fig. 1 was studied in a previous paper.[1] In the present paper we investigate the structure, conformation and dynamics of VCB using X-ray and multinuclear NMR techniques.

NMR relaxation parameters such as the nuclear Overhauser effect (NOE) and the spin–lattice relaxation time (T_1) are powerful tools for structure and conformation determinations, especially in solution, because they depend on the inverse sixth power of internuclear distances. Information about the stereochemistry in solution may also be obtained from chemical shifts and coupling constants.

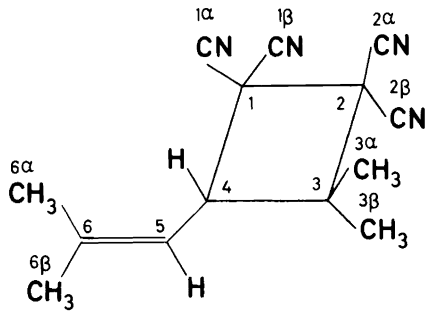

Fig. 1. Depiction of the VCB molecule showing the labelling of the carbon atoms. Note that the vinyl carbons have been labelled 5 and 6 instead of 1′ and 2′.

The stereochemistry of cyclobutane derivatives has been extensively reviewed by Moriarty[2] and Allen.[3] Vicinal substituents are maximally eclipsed in the planar form, but repulsion is reduced by ring puckering. The ring geometry of VCB should reflect the delicate balance between ring-strain forces and the repulsive interactions between the vicinal substituents. The puckered form of cyclobutane is preferred, but only by ca. 5.9 kJ mol^{-1} over the planar form.[4] This energy barrier is of the same order of magnitude as the crystal packing forces. It is therefore no accident that the only clear characterization of planar cyclobutanes occurs in the crystalline state.[3]

The main objective of this work was to determine the crystal structure of VCB using X-ray diffraction and to investigate the solution conformation and dynamics using NOE and T_1 NMR measurements.

Experimental

Sample preparation. VCB was synthesized from commercial tetracyanoethylene and 2,5-dimethyl-2,4-hexadiene in chloroform solution as described by Asaad and Aksnes.[1]

X-Ray diffraction. The determination of the unit cell parameters and data collection were carried out on an

* To whom correspondence should be addressed.

ENRAF-NONIUS CAD4 diffractometer using monochromated Mo $K\alpha$ radiation ($\lambda = 0.71073$ Å). The crystal was cut to approximately orthorhombic shape, 0.08×0.13×0.18 mm^3. The temperature at the crystal site was 90 ± 1 K. The cell parameters are based on a least-squares fit to diffractometer settings for 22 general reflections with $2\theta > 20°$. The crystal structure is orthorhombic, $a = 7.470(2)$, $b = 11.446(2)$, $c = 30.862(5)$ Å; $V = 2638.7(1.4)$ Å^3; $M = 238.29$ a.m.u.; $z = 8$; $d_x = 1.200$ g cm^{-3}; $mu = 0.702$ cm^{-1}; $F(000) = 1008$; space group *Pcab* (No. 61). All unique reflections with $2\theta \leq 50°$ were sampled. The intensities were collected using the ω-scan technique with a constant scan speed of 2.5° min^{-1}, minimum scan width 1.5°, including 2×0.25° for background counts. Three standard reflections were measured every hour and the data later corrected accordingly; the minimum and maximum corrections were 0.97 and 1.08. The orientation of the mounted crystal was checked every 200 reflections. Out of the 2316 possible reflections, 1403 with $I > 2\sigma(I)$ were included in the structure analysis. The MULTAN computer program gave all non-hydrogen atom positions; hydrogen atoms were located by difference Fourier syntheses. Least-squares refinement with isotropic thermal parameters preceded the empirical absorption correction,[5] minimum and maximum corrections were 0.90 and 1.03 (average 0.99). The least-squares refinement (including anisotropic thermal parameters for non-hydrogen atoms), minimizing $w(F_o - F_c)^2$, where $w = 4LpI/[\sigma^2(I) + (0.02\ I)^2]$ and $I = I_{count}$, converged with $R = 4.56\%$, $R_w = 3.32\%$ and $S = 1.259$. The final difference electron density map showed maximum and minimum values of 0.214 and −0.257 e Å^{-3}. Secondary extinction effects were found to be negligible. The programs used were ENRAF-NONIUS' Structure Determination package 1987.

NMR spectra. A ca. 0.5 M solution in chloroform-d and a ca. 2 M solution in acetone-d_6 were prepared in 5 and 10 mm o.d. NMR tubes, respectively. Both NMR tubes were degassed by several freeze–pump–thaw cycles and sealed under vacuum. The ^{1}H, ^{13}C and ^{15}N spectra were obtained at 400.13, 100.62 and 40.55 MHz, respectively, on a Bruker AM 400 WB spectrometer. The 10 mm NMR tube was only used for the ^{15}N NMR measurements. The digital resolutions of the 1D NMR spectra were 0.097, 0.152 and 0.086 Hz per point for the ^{1}H, ^{13}C and ^{15}N spectra, respectively.

The homonuclear Overhauser enhancements were measured by means of NOE difference spectroscopy. One frequency list was used to define all on-resonance irradiation points and one off-resonance point. Subtraction of the unperturbed from the perturbed FID, followed by Fourier transformation and integration, yielded the NOE values listed later in Table 4. Selective pre-irradiation of protons 3α, 3β, 4 and 5, however, gave no measurable ^{15}N NOE intensity differences relative to an off-resonance ^{1}H irradiated spectrum.

The carbon–proton chemical shift correlations were established using the following heteronuclear shift correlation (HSC) pulse sequence (^{1}H-irradiation in parentheses):[6] [RD(off)-(90°)-t_1/2-180°−t_1/2-τ-90°(90°)-τ/2-t_2(BB)]. The relaxation delay, RD, was 8 s, and the experiemnt was optimized for the methyl carbons with $^1J(^{13}C-^1H)$ = 127 Hz by setting τ = 3.94 ms. We recorded 256 FIDs in t_1 and 2K data points in t_2. The spectral widths were ± 1016 Hz in f_1 and 14285 Hz in f_2.

The following pulse sequence was used in the *J*-resolved experiment (^{1}H-irradiation in parentheses):[7] [RD(BB)-90° (off)-t_1/2-180°(selective 180°)-t_1/2-t_2(BB)]. RD was 10 s and the decoupler power was calibrated to give a selective 180° proton inversion pulse of 9.47 ms duration ($\gamma B_2/2\pi$ = 26 Hz, see below). We recorded 64 FIDs in t_1 and 4K data points in t_2. The spectral widths were ±6.01 Hz in f_1 and 14285 Hz in f_2. All 2D FIDs were zero-filled in both dimensions, multiplied by a sine-bell function prior to Fourier transformation, and processed in the absolute value mode.

The T_1 measurements were performed using an ordinary inversion–recovery pulse sequence [RD-180°-t_1-90°-t_2]. For the ^{1}H measurements one scan was acquired for each of 12 variable t_1 values with RD = t_1 (max) = 15 s. For the ^{13}C measurements, 16 scans were accumulated for each of 21 variable t_1 values with RD = t_1 (max) = 100 s. The superfast-inversion–recovery (SUFIR) method[8] was used to get an estimate of the ^{15}N relaxation times, followed by an ordinary inversion–recovery experiment. 32 scans were accumulated for each of 11 variable t_1 values with RD = t_1 (max) = 80 s. A non-linear three-parameter fitting of peak heights was used for calculating the T_1 values from the experimental data.

The central carbon signal and the residual proton signal of chloroform-d were used as secondary references for the ^{13}C and ^{1}H chemical shifts (77.0 and 7.2 ppm from TMS). The ^{15}N chemical shifts were measured relative to external nitromethane at 380 ppm (20 % v/v in acetone-d_6).

A sample containing trichloroethylene in acetone-d_6 was prepared, and the ^{13}C doublet due to the two-bond $^{13}C-^1H$ coupling (8.49 Hz) was used to calibrate the soft ^{1}H decoupler pulse ($\gamma B_2/2\pi = 26$ Hz) following a procedure due to Bax and Freeman.[7]

The simulations of the ^{1}H and ^{13}C spectra were performed by means of the PANIC program available in the Bruker Software Library.

Results and discussion

Solid-state structure. An ORTEP drawing of the VCB molecule is shown in Fig. 2. The bond lengths and angles are calculated from the coordinates in Table 1 and listed in Tables 2 and 3. The variation in the C−C bond lengths of the heptasubstituted ring system from 1.563 Å for C3–C4 to 1.603 Å for C1–C2 is ascribed to steric effects, in particular non-bonded interactions between vicinal substituents. The C1–C2 and C2–C3 bond lengths of 1.602–1.603 Å represent a considerable elongation by comparison with the electron diffraction value in the parent compound (1.548 Å)[9] or with the X-ray means for a large number of

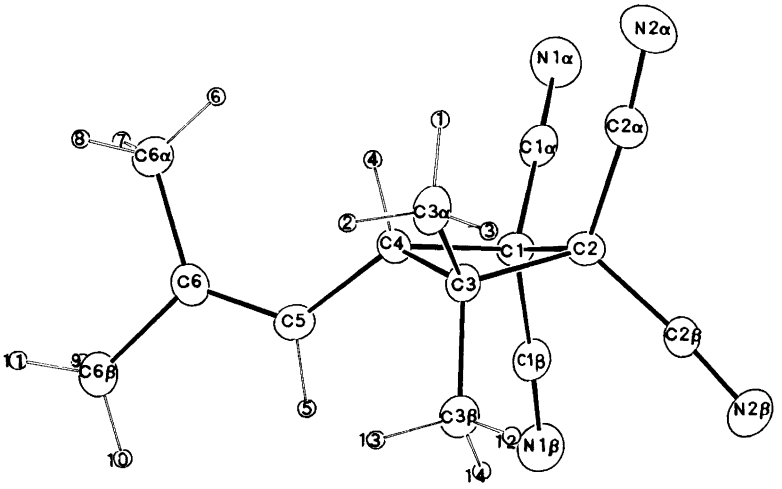

Fig. 2. ORTEP drawing of the VCB molecule. Note that the atom symbol (H) has been omitted when labelling the hydrogen atoms.

Table 1. Final atomic parameters and their standard deviations. Asterisks denote isotropic refinement. Anisotropically refined atoms are given in the form of the isotropic equivalent thermal parameter.

Atom[a]		*x*	*y*	*z*	*B*/Å²[b]
N1α		0.5067(3)	−0.2618(2)	0.16044(6)	2.49(4)
N1β		0.7614(3)	0.0731(2)	0.14747(6)	2.10(4)
N2α		0.2832(3)	−0.2479(2)	0.05696(6)	2.67(4)
N2β		0.6881(3)	0.0256(2)	0.02822(6)	1.88(4)
C1		0.4806(3)	−0.0523(2)	0.12801(7)	1.24(4)
C1α		0.4984(3)	−0.1693(2)	0.14645(7)	1.58(5)
C1β		0.6403(2)	0.0167(2)	0.13856(7)	1.42(5)
C2		0.4299(3)	−0.0494(2)	0.07754(7)	1.23(5)
C2α		0.3523(3)	−0.1612(2)	0.06423(7)	1.65(5)
C2β		0.5757(3)	−0.0119(2)	0.04917(7)	1.18(4)
C3		0.2817(3)	0.0470(2)	0.08896(7)	1.36(5)
C3α		0.0973(3)	0.0267(2)	0.06943(7)	1.75(5)
C3β		0.3491(3)	0.1686(2)	0.07760(7)	1.73(5)
C4		0.2986(3)	0.0138(2)	0.13790(7)	1.29(4)
C5		0.3021(3)	0.1078(2)	0.17118(7)	1.54(5)
C6		0.2163(3)	0.1079(2)	0.20884(7)	1.34(5)
C6α		0.1003(3)	0.0119(2)	0.22561(7)	1.78(5)
C6β		0.2337(3)	0.2110(2)	0.23868(7)	1.89(5)
H1	H3α	0.060(3)	−0.059(2)	0.0765(6)	2.6(5)*
H2		0.008(3)	0.078(2)	0.0834(7)	3.0(5)*
H3		0.102(3)	0.039(2)	0.0368(7)	2.8(6)*
H4		0.208(3)	−0.048(2)	0.1440(6)	2.0(5)*
H5		0.369(3)	0.177(2)	0.1633(6)	1.8(5)*
H6	H6α	0.099(3)	−0.060(2)	0.2074(6)	2.9(6)*
H7		0.135(3)	−0.010(2)	0.2555(7)	2.8(5)*
H8		−0.023(3)	0.039(2)	0.2312(7)	3.9(6)*
H9	H6β	0.294(3)	0.184(2)	0.2669(6)	2.5(5)*
H10		0.303(3)	0.276(2)	0.2257(6)	2.3(5)*
H11		0.117(3)	0.241(2)	0.2488(7)	3.6(5)*
H12	H3β	0.350(3)	0.181(2)	0.0464(7)	3.2(6)*
H13		0.269(3)	0.228(2)	0.0911(6)	1.6(5)*
H14		0.475(3)	0.187(2)	0.0890(6)	2.1(5)*

[a]The X-ray and NMR labelling is the same unless otherwise stated.

[b]$B_{eq} = \frac{4}{3} \sum_i \sum_j a_i a_j \beta_{ij}$.

tetrasubstituted C1–C2 fragments of cyclobutane rings (1.575 Å).[3] The ring $-CH_3$ bond lengths (1.521–1.522 Å) are similar to values reported for C(sp^3) substituents on a number of cyclobutane rings (1.52–1.53 Å).[3]

We define the angle of pucker (φ) as the complement of the dihedral angle between the planes through C1–C2–C3 and C3–C4–C1. The repulsion between the vicinal substituents of VCB is reduced by a small ring puckering (φ = 21.8°) accompanied by a decrease in the C1–C2–C3 valence angle (θ) from 90 to 87.9°. The angle of pucker is well within the range reported for a large number of cyclobutane rings with acyclic substituents (16–30°).[3] The increase of the intra-ring strain with decreasing θ (or increasing φ) is nearly counterbalanced by movement of the vicinal substituents out of the eclipsed positions.

The torsional angles (τ) between the cyano substituents, e.g. τ(C1α–C1–C2–C2α), are somewhat larger (18.3–19.6°) than the intra-ring torsional angle τ(C4–C1–C2–C3) =

Table 2. Bond distances with estimated standard deviations in parentheses.

Bond	Distance/Å	Bond	Distance/Å
N1α–C1α	1.144(3)	C6–C6α	1.493(3)
N1β–C1β	1.145(3)	C6–C6β	1.502(3)
N2α–C2α	1.141(3)	C3α–H1	1.04(2)
N2β–C2β	1.143(2)	C3α–H2	0.99(2)
C1–C1α	1.462(3)	C3α–H3	1.02(2)
C1–C1β	1.467(3)	C3β–H12	0.97(2)
C1–C2	1.603(3)	C3β–H13	1.00(2)
C1–C4	1.586(3)	C3β–H14	1.03(2)
C2–C2α	1.464(3)	C4–H4	1.00(2)
C2–C2β	1.462(3)	C5–H5	0.97(2)
C2–C3	1.602(3)	C6α–H6	1.00(2)
C3–C3α	1.522(3)	C6α–H7	0.99(2)
C3–C3β	1.521(3)	C6α–H8	0.98(3)
C3–C4	1.563(3)	C6β–H9	1.03(2)
C4–C5	1.487(3)	C6β–H10	0.99(2)
C5–C6	1.327(3)	C6β–H11	0.99(2)

Table 3. Bond angles with estimated standard deviations in parentheses.

Bond	Angle/°	Bond	Angle/°
C1α–C1–C1β	109.4(2)	N2β–C2β–C2	174.9(2)
C1α–C1–C2	114.8(2)	C2–C3–C3α	115.7(2)
C1α–C1–C4	116.1(2)	C2–C3–C3β	110.5(2)
C1β–C1–C2	113.4(2)	C2–C3–C4	89.4(2)
C1β–C1–C4	113.4(2)	C3α–C3–C3β	110.4(2)
C2–C1–C4	88.6(2)	C3α–C3–C4	114.8(2)
N1α–C1α–C1	177.7(3)	C3β–C3–C4	114.7(2)
N1β–C1β–C1	177.7(2)	C1–C4–C3	89.9(2)
C1–C2–C2α	110.4(2)	C1–C4–C5	117.6(2)
C1–C2–C2β	114.4(2)	C3–C4–C5	119.6(2)
C1–C2–C3	87.9(2)	C4–C5–C6	126.7(2)
C2α–C2–C2β	112.5(2)	C5–C6–C6α	125.7(2)
C2α–C2–C3	113.0(2)	C5–C6–C6β	119.8(2)
C2β–C2–C3	116.4(2)	C6α–C6–C6β	114.6(2)
N2α–C2α–C2	174.2(3)		

Table 4. Homonuclear Overhauser enhancements (NOEs) and inter-nuclear H···H distances.

Interaction vector	NOE[a] /%	Average H···H distance/Å	
		X-Ray	NMR
H4···H3α	20.80	2.90[b]	2.90[b]
H4···H3β	3.01	3.83	3.99
H4···H6α	19.16	3.00	2.94
H4···H6β	0.57	4.64	5.29
H5···H3α	1.50	4.32	4.50
H5···H3β	23.02	2.82	2.85
H5···H6α	~0	3.85	–
H5···H6β	18.55	2.95	2.96

[a]NOEs of H4 or H5 upon selective irradiation of the methyl resonances. [b]This internuclear distance was used as internal reference.

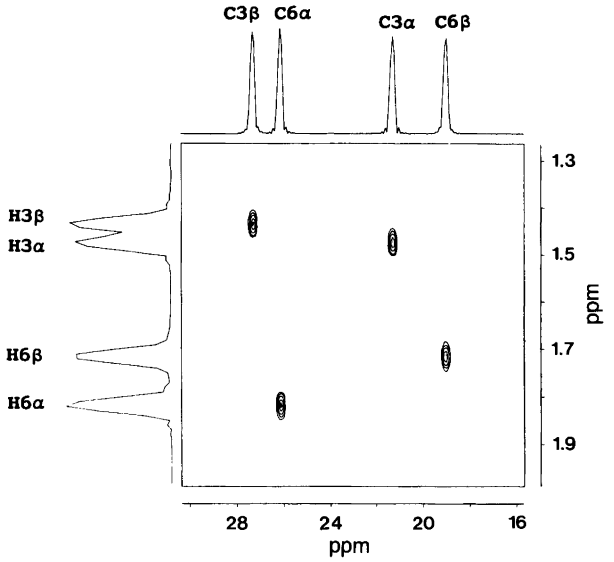

Fig. 3. Two-dimensional heteronuclear shift correlation spectrum of the methyl region in VCB.

15.1°, thereby causing a further reduction of the steric repulsion between these substituents. The vicinal 2-cyano and 3-methyl substituents in the α position experience a similar rocking in opposite senses in that τ(C2α–C2–C3–C3α) = −21.5° compared with an intra-ring torsional angle of −15.40°. In practice the experimental values of τ for 1,2-disubstituted rings are generally larger than values of the intra-ring torsional angle, especially for highly puckered rings.[3] The conformation about C4–C5 is *anti*, with the torsional angle τ(H4–C4–C5–H5) = 167.6°.

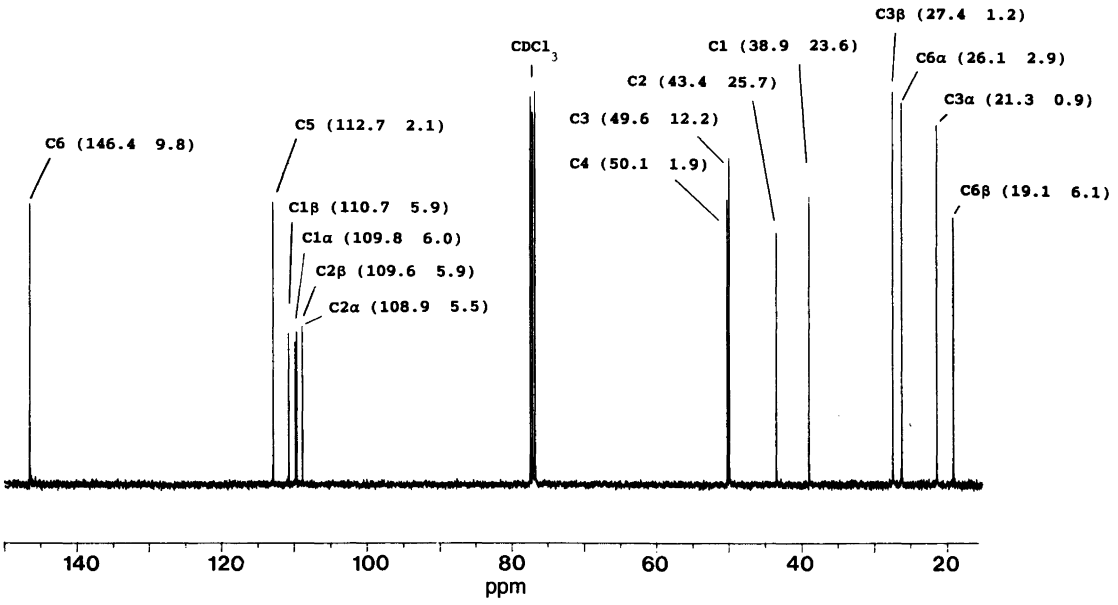

Fig. 4. CPD decoupled ^{13}C NMR spectrum of VCB. The chemical shifts (in ppm from TMS) and T_1 values (in s) are given in parentheses.

Table 5. 400 MHz ^{1}H NMR parameters of VCB at 293 K.

Chemical shifts (ppm from TMS)		Coupling constants/Hz[a]		Spin–lattice relaxation times/s	
δ(H4)	3.753	^3J(H4, H5)	9.670	T_1(H4)	3.1
δ(H5)	5.278	^4J(H4, H3α)	0.41[b]	T_1(H5)	3.4
δ(H3α)	1.482	^4J(H5, H6α)	1.437	T_1(H3α)	0.8
δ(H3β)	1.445	^4J(H5, H6β)	1.433	T_1(H3β)	1.0
δ(H6α)	1.827	^4J(H6α, H6β)	0.316	T_1(H6α)	1.8
δ(H6β)	1.724	^5J(H4, H6α)	0.289	T_1(H6β)	2.6

[a]The probable error is ≤ 0.005. [b]From long-range COSY.

Assignment of NMR spectra. Although the 400 MHz ^{1}H spectrum of VBC is quite simple, the assignment of the four methyl resonances is not straightforward. For the unambiguous assignment of the methyl region a homonuclear NOE difference experiment was performed (Table 4). The corresponding methyl carbon resonances were then assigned by running a 2D heteronuclear shift correlation experiment as shown in Fig. 3. It is noteworthy that the ^{1}H and ^{13}C chemical shifts of the methyl substituents appear in a different order. The assignments of the remaining carbon resonances are based on chemical shift arguments, analyses of coupling patterns and selective proton irradiation. The composite pulse decoupled (CPD) ^{13}C spectrum of VCB is shown in Fig. 4, together with the chemical shifts and T_1 values. The ^{1}H–^{1}H and ^{1}H–^{13}C coupling constants listed in Tables 5 and 6 were obtained from iterative computer analysis unless otherwise stated.

The ^{15}N spectrum of VCB shown in Fig. 5 was assigned on the basis of selective proton irradiation and chemical shift arguments. Unfortunately, selective pre-irradiation of protons 3α, 3β, 4 and 5 had no measurable effect on the intensity of the ^{15}N transitions.

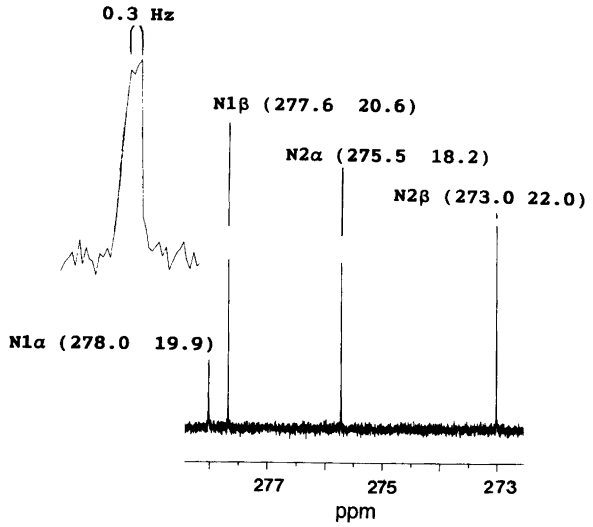

Fig. 5. CPD decoupled ^{15}N NMR spectrum of VCB. The chemical shifts (in ppm from nitrometane at 380 ppm) and T_1 values (in s) are given in parentheses.

Solution conformation. The ^{1}H and ^{13}C NMR spectra were studied to determine the solution conformation of VCB. The homonuclear NOE difference data listed in Table 4 show that the *anti* configuration of the vinyl group persists in solution, but it is not clear to what extent the ring-puckering is constant. The NOE data give somewhat larger values for the H4–H6β and H5–H3α distances than the X-ray data. This difference is largely ascribed to experimental inaccuracy, since enhancements of less than 1–2 % are hard to measure reliably. The spin coupling constants also provide some information about the conformation in solution. Thus the large value of the vicinal coupling constant involving H4 and H5 (9.67 Hz) indicates that those protons have an *anti* relationship in solution as well as in

Table 6. ^{13}C–^{1}H coupling constants (in Hz)[a] of VCB at 293 K.

Carbon	Proton: 3α	3β	4	5	6α	6β
1[b]			4.41[c]	3.47[c]		
1α			7.63	0.38[c]		
1β			6.10	0[c]		
2	6.571	6.472	1.343	0.163		
2α			0.65	0[c]		
2β			0[c]	0[c]		
3[b]			4.51[c]	1.97[c]		
3α	128.443	4.882	4.909	0.234		
3β	4.304	129.308	4.300	−0.008		
4[b]			139.94	3.19[c]	1.25[c]	
5			−4.747	157.919	6.214	4.893
6			4.241	−1.307	−6.216	−6.212
6α			−0.003	7.762	126.620	4.138
6β			0.611	6.626	4.267	126.867

[a]The probable error is ≤ 0.016. [b]Unresolved multiplet; not amenable to spectral analysis. [c]From selective *J*-resolved 2D. The sign is not determined.

the solid state, where the torsional angle τ(H4–C4–C5–H5) = 167.6°.

The ^3J(C, H) coupling constants also show all the orientation phenomena found in the corresponding ^{1}H–^{1}H coupling constants. The small value of ^3J(C2, H4) (1.34 Hz) thus indicates that the appropriate torsional angles of the two coupling paths are around 90°, in agreement with the solid-state structure for which τ(H4–C4–C1–C2) = 92.7° and τ(H4–C4–C3–C2) = 88.9°.

The one-bond coupling constant ^1J(C, H) increases from 136 Hz in the parent cyclobutane[10] to 139.9 Hz in VCB. The positive contribution of 3.9 Hz is largely ascribed to hybridization changes of the coupled carbon. For simple hydrocarbons there is a clear consistency between the trend in the mean C–R bond length and changes in ^1J(C, H). The percentage *s*-character of the coupled carbon bonds can be estimated from the relation s (%) = 0.20 ^1J(C, H). This proportionality was first proposed by Muller and Pritchard,[11] but there is now a body of evidence to show that this empirical relation has a good theoretical basis for simple hydrocarbons[12,13] and for a range of small-ring compounds.[14] By using this empirical relation we find that the *s*-character increases from 27 % in cyclobutane to 28 % in VCB. The observation that the exocyclic C4–C5 bond length of VCB (1.487 Å) is significantly shorter than the mean bond length reported for a series of C(sp^2)-substituted cyclobutanes (1.504 Å)[3] indicates that the variation of ^1J(C, H) can largely be ascribed to hybridization changes.

T_1 relaxation times. The measured ^{1}H and ^{13}C T_1 times are given in Table 5 and Fig. 4, respectively. The motional characteristics of VCB are most conveniently studied on the basis of the ^{13}C T_1 data because the ^{1}H T_1 relaxation times, in contrast to the ^{13}C T_1 times, receive significant contributions from intermolecular interactions. At 293 K the proton-bearing carbons of VCB show maximum NOE enhancements within experimental error. It follows that the T_1 relaxation of these carbons is governed by the dipole–dipole mechanism. For mobile liquids the dipolar ^{13}C relaxation rate is given by eqn. (1),[15] where n_H is the number of protons directly attached to the carbon in question, r_{CH} is the C–H bond length and τ_{eff}^{CH} is the effective correlation time for the molecular reorientation. For carbons C4 and C5 $\tau_{eff}^{CH} = \tau_r$, the correlation time for the overall motion of the molecule. Since T_1 values for C4 and C5 are equal within experimental error, the whole-molecule motion is assumed to be isotropic. For the methyl carbons, however, one must also take into account the internal methyl rotation with correlation time τ_m. By assuming that the overall and internal motions are independent of each other and that the latter motion occurs by random jumps between three equilibrium positions, it is readily shown that eqn. (2) holds.[16] The correlation times τ_r and τ_m were obtained from the experimental T_1(^{13}C) data by using eqns. (1) and (2). It was assumed that all methyl carbons had tetrahedral geometry in solution and the C–H bond length was normalized to 1.09 Å. When calculating that τ_r = 23 ps we used the mean T_1 value for C4 and C5 (2.0 s).

$$\frac{1}{T_1(^{13}C)} = \left(\frac{\mu_0}{4\pi}\right)^2 n_H \gamma_H^2 \gamma_C^2 \hbar^2 r_{CH}^{-6} \tau_{eff}^{CH} \quad (1)$$

$$\tau_{eff}^{CH} = \frac{1}{9}\tau_r + \frac{8}{9}\left(\frac{1}{\tau_r} + \frac{1}{\tau_m}\right)^{-1} \quad (2)$$

By using this τ_r value and the appropriate T_1(^{13}C) values for the methyl carbons, τ_m correlation times of 69, 25 and 3.7 ps were obtained for the 3α, 3β and 6α carbons, respectively. τ_m is not obtainable from the T_1(^{13}C) value for the 6β methyl group because $\tau_{eff}^{CH} \approx \tau_r/9$, i.e. $\tau_m \ll \tau_r$.

The intra-CH_3 dipolar contributions to the T_1(^{1}H) relaxation times were calculated by using the correlation times obtained from the T_1(^{13}C) values. The calculated T_1(^{1}H) values were 0.2–0.6 s longer (ca. 20 %) than the experimental values. Intramolecular CH_3–CH_3 dipolar interactions contribute another 5–10 % to the ^{1}H relaxation,[15] whereas intermolecular interactions are responsible for the remaining contribution. The C_3 rotation of the methyl groups at C6 is an order of magnitude faster than both the C_3 rotation of the methyl groups at C3 and the overall molecular tumbling. This observation indicates, in accordance with the solid-state structure, that the rotation of the 3β and, in particular, the 3α methyl groups is sterically hindred. It is thus found that the intramolecular nonbonded distance between H1 and N2α (2.8 Å) is very close to the corresponding sum of the van der Waals' radii (2.7 Å).

The relatively short T_1 times observed for the cyano carbons (5.5–6.0 s) and nitrogens (18.2–22.0 s), and the absence of the NOE effect, indicate that the relaxation is dominated by the shielding anisotropy mechanism modulated by the overall molecular tumbling.[15] If we assume that the shielding of the CN group is axially symmetric and use the previously obtained value for τ_r (23.3 ps) and the mean value for T_1 of the cyano carbons (5.8 s), a shielding anisotropy Δσ of 372 ppm is obtained. This shielding anisotropy is fairly close to the experimental and theoretical values reported for HCN (282 and 295 ppm, respectively) and the theoretical value for CH_3CN (290 ppm).[17,18]

Acknowledgement. We are grateful to The Norwegian Research Council for Science and the Humanities (NAVF) for support through a fellowship grant to T. B.

References

1. Asaad, A. N. and Aksnes, G. *Z. Naturforsch. Teil A 43* (1988) 435.
2. Moriarty, R. M. In: Eliel, E. L. and Allinger, N. L., Eds., *Topics in Stereochemistry,* Wiley, New York 1974, Vol. 8, pp. 271–421.
3. Allen, F. H. *Acta Crystallogr., Sect. B 40* (1984) 64.

4. Stone, J. M. R. and Mills, I. M. *Mol. Phys. 18* (1970) 631.
5. Walker, N. and Stuart, D. *Acta Crystallogr., Sect. A 39* (1983) 158.
6. Bax, A. and Morris, G. *J. Magn. Reson. 42* (1981) 501.
7. Bax, A. and Freeman, R. *J. Am. Chem. Soc. 104* (1982) 1099.
8. Canet, D., Brondeau, J. and Elbayed, K. *J. Magn. Reson. 77* (1988) 483.
9. Almenningen, A., Bastiansen, O. and Skancke, P. N. *Acta Chem. Scand. 15* (1961) 711.
10. Burke, J. J. and Lauterbur, P. C. *J. Am. Chem. Soc. 86* (1964) 1870.
11. Muller, N. and Pritchard, D. W. *J. Chem. Phys. 31* (1959) 768, 1471.
12. Newton, M. D., Schulman, J. M. and McManus, M. M. *J. Am. Chem. Soc. 96* (1974) 17.
13. Ellis, P. D. and Ditchfield, R. In: Levy, G. C., Ed., *Topics in Carbon-13 NMR Spectroscopy*, Wiley, London 1976, pp. 433–476.
14. Ellis, P. D. and Maciel, G. E. *J. Am. Chem. Soc. 92* (1970) 5829.
15. Levy, G. C., Lichter, R. L. and Nelson, G. L. *Carbon-13 Nuclear Magnetic Resonance Spectroscopy*, Wiley, New York 1980, pp. 213–223.
16. Aksnes, D. W. and Ramstad, K. *Magn. Reson. Chem. 25* (1987) 534.
17. Appleman, B. R., Dailey, B. P. and Waugh J. S. *Adv. Magn. Reson. 7* (1974) 231.
18. Millett, F. and Dailey, B. P. *J. Chem. Phys. 54* (1971) 5434.

Received May 16, 1990.